

Full-Wave Characterization of Microstrip Open End Discontinuities Patterned on Anisotropic Substrates Using Potential Theory

S. S. Toncich, *Senior Member, IEEE*, R. E. Collin, *Fellow, IEEE*, and K. B. Bhasin, *Senior Member, IEEE*

Abstract—A technique for the full-wave characterization of microstrip discontinuities fabricated on uniaxial anisotropic substrates using a dynamic source reversal method based on potential theory is presented. The dynamic source reversal technique was introduced in 1989 by R. E. Collin and S. S. Toncich [1]. The open end discontinuity is enclosed in a cut-off waveguide of infinite extent, with the anisotropic axis aligned perpendicular to the air-dielectric interface. A full description of the sources on the microstrip line is included with proper edge conditions built in. The resulting computer program is written in compiled BASIC and is intended for execution on personal computers possessing minimal memory and/or processing resources. Extension to other discontinuities is discussed.

INTRODUCTION

WHILE there is extensive data available on the microwave characterization of a variety of microstrip discontinuities using both quasi-static [2–4] and full-wave techniques [5–7], the characterization has been restricted to isotropic substrates. To date, there is no published data regarding the frequency dependent characterization of microstrip discontinuities patterned on anisotropic substrates. Some very useful microwave substrates however, specifically sapphire, are anisotropic and so any discontinuity structures fabricated on them cannot be properly characterized by the techniques that have been developed for isotropic dielectric substrates.

A technique for the full-wave characterization of microstrip open ends fabricated on lossless uniaxial anisotropic substrates has been developed and is presented here. It is based on a dynamic source reversal technique that uses potential theory [8], which is a generalization of the charge reversal technique introduced several years ago [2]. The discontinuity is enclosed in a waveguide of infinite extent whose dimensions are such that the guide is cut off for the propagating frequency of the dominant microstrip mode. All sources on the microstrip are represented, and

the technique does not require a model for the source excitation. The electric fields inside the waveguide are obtained exclusively in terms of the sources on the microstrip line and the scalar, rather than dyadic Green's functions. These features combined to provide for accurate modeling of the discontinuity along with substantial computational savings over other techniques. This is important in computer aided design programs where many iterations are often required to obtain desired circuit performance.

DYNAMIC SOURCE REVERSAL TECHNIQUE

The anisotropic axis of the substrate is aligned perpendicular to the air-dielectric interface as shown in Fig. 1. The anisotropic dielectric may be represented as a tensor quantity given by

$$\kappa(y) = \kappa(y) \mathbf{l} + [\kappa_y(y) - \kappa(y)] \mathbf{a}_y \mathbf{a}_y \quad (1)$$

where \mathbf{l} is the unit dyad, and $\kappa(y) = \kappa_y(y) = 1$ for $y > h$. The microstrip line is assumed to be infinitely thin and located at a height $y = h^+$. The sources on the line are the longitudinal and transverse currents, J_z and J_x , respectively, and the charge, ρ . In terms of these sources, the scalar and vector potentials, Φ and \mathbf{A} , respectively, for the dielectric loaded waveguide may be determined from

$$(\nabla^2 + \kappa k_0^2) A_x = -\mu_0 J_x \quad (2)$$

$$(\nabla^2 + \kappa k_0^2) A_z = -\mu_0 J_z \quad (3)$$

$$(\nabla^2 + \kappa_y k_0^2) A_y = j\omega \mu_0 \epsilon_0 (\kappa - 1) \Phi (h) \delta(y - h) + j\omega \mu_0 \epsilon_0 (\kappa_y - \kappa) \partial \Phi / \partial y \quad (4)$$

$$[\kappa (\partial^2 / \partial x^2 + \partial^2 / \partial z^2) + \partial (\kappa(y) \partial / \partial y) / \partial y + \kappa^2(y) k_0^2] \Phi = -\rho / \epsilon_0 + j\omega (\kappa_y - 1) A_y (h) \delta(y - h) - j\omega (\kappa_y - \kappa) \partial A_y / \partial y \quad (5)$$

where the Lorentz condition, $\nabla \cdot \mathbf{A} = -j\omega \mu_0 \epsilon_0 \kappa(y) \Phi$ along with $\partial \kappa(y) / \partial y = -(\kappa - 1) \delta(y - h)$ have been used to obtain (2)–(5) [9]. The potentials appearing in (2)–(5) are obtained from the appropriate Green's functions and

Manuscript received March 22, 1993; revised June 11, 1993.

S. S. Toncich performed this work while an NRC Research Associate at NASA Lewis Research Center, Cleveland, OH 44135. He is now with Bird Electronic Corporation, Solon, OH 44139.

R. E. Collin is with the Department of Electrical and Applied Physics, Case Western Reserve University, Cleveland, OH 44106.

K. B. Bhasin is with NASA Lewis Research Center, Cleveland, OH 44135.

IEEE Log Number 9212969.

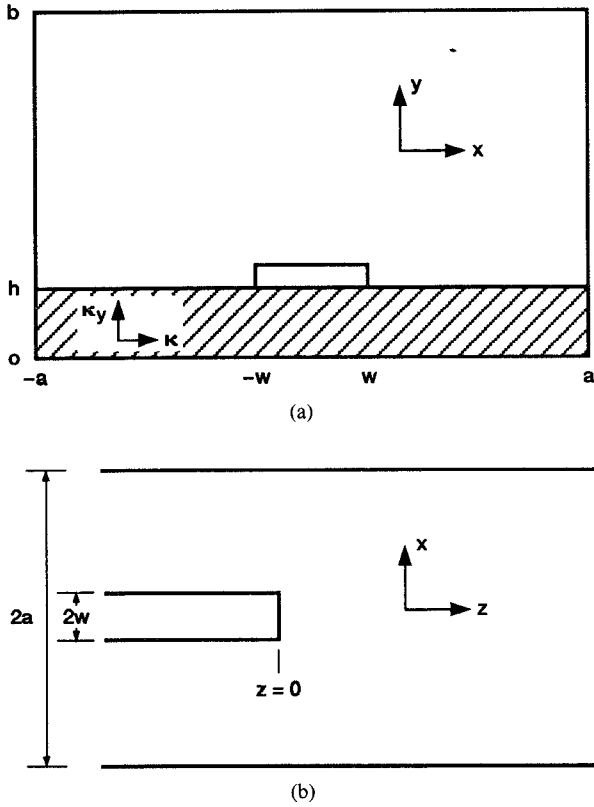


Fig. 1. Shielded microstrip geometry. (a) Front view (b) Top view.

the corresponding sources using

$$A_{x,z}(x, h, z) = \mu_0 \int_{z'} \int_{x'} G_{x,z}(x, h, z; x', h, z') \cdot J_{x,z}(x', h, z') dx' dz' \quad (6)$$

$$\epsilon_0 \Phi(x, h, z) = \int_{z'} \int_{x'} G(x, h, z; x', h, z') \cdot \rho(x', h, z') dx' dz'. \quad (7)$$

Expressions for the Green's functions corresponding to the geometry shown in Fig. 1 may be obtained in the following manner. G_x and G_z must satisfy the following expression

$$(\nabla^2 + \kappa k_0^2) G_{x,z} = -\delta(x - x')\delta(y - h)\delta(z - z'). \quad (8)$$

Expressions for the Green's functions will be obtained using a Fourier transform method. Assuming a general solution for $G_{x,z}$ of the form

$$G_{x,z} = (1/2\pi) \sum_{n=1}^{\infty} \int_{-\infty}^{\infty} \varphi_n(x) f_n(y) e^{-j\omega z} d\omega \quad (9)$$

where

$$\varphi_n(x) = \begin{cases} \cos(u_n x) & \text{for } G_z \\ \sin(u_n x) & \text{for } G_x \end{cases}$$

and $u_n = n\pi/2a$ for n odd, and the y dependence is of

the form

$$f_n(y) = A_n \sin(pc) \sin(ly), \quad y < h \quad (10a)$$

$$f_n(y) = A_n \sin(lh) \sin(p(b - y)), \quad y > h \quad (10b)$$

Substituting (9), (10a) and (10b) into (8) and performing the required calculations, gives the Green's function components as

$$G_{x,z}(x, h, z; x', h, z') = (1/2\pi) \sum_{n=1}^{\infty} \int_{-\infty}^{\infty} \varphi_n(x, x') DZ_n \sin(pc) \cdot \sin(lh) e^{-j\omega(z-z')} d\omega \quad (11)$$

where

$$\begin{aligned} \varphi_n(x, x') &= \cos(u_n x) \cos(u_n x') & \text{for } G_z \\ \varphi_n(x, x') &= \sin(u_n x) \sin(u_n x') & \text{for } G_x \\ DZ_n &= 1/a(p \sin(lh) \cos(pc) \\ &\quad + l \sin(pc) \cos(lh)) \end{aligned} \quad (12)$$

and the l 's and p 's are related by $p^2 = k_0^2 - \omega^2 - u_n^2$, $l^2 = \kappa k_0^2 - \omega^2 - u_n^2$.

The expressions for G and G_y , corresponding to Φ and A_y , respectively, are more complicated since these expressions are coupled. As a result, they must be solved simultaneously. However, solutions for G_y and G may be obtained in a somewhat easier fashion by noticing that

$$G_y(x, h, z; x', h, z') = (1/2\pi) \int_{-\infty}^{\infty} \cdot g_y(x, h, \beta; x', h, z') e^{j\beta z} d\beta \quad (13)$$

$$G(x, h, z; x', h, z') = (1/2\pi) \int_{-\infty}^{\infty} \cdot f(x, h, \beta; x', h, z') e^{j\beta z} d\beta \quad (14)$$

where $g_y(\cdot)$ and $f(\cdot)$ are the Green's functions calculated for a z dependence of $e^{-j\beta z}$ in [9], for an infinite microstrip line with side walls, but not top cover. With a top cover in place, the y dependence is chosen to be of the form

$$f_n(y) = \begin{cases} A_{1n} \sin(l_1 y) + A_{2n} \sin(l_2 y), & y < h \\ A_{3n} \sin(p(b - y)) & y > h \end{cases} \quad (15a)$$

and

$$g_n(y) = \begin{cases} B_{1n} \cos(l_1 y) + B_{2n} \cos(l_2 y), & y < h \\ B_{3n} \cos(p(b - y)) & y > h \end{cases} \quad (15b)$$

instead of the decaying exponential functions used in [9].

The eigenvalues for this configuration are, for $y < h$

$$l_1^2 = \kappa k_0^2 - \gamma_n^2 \quad (16a)$$

$$l_2^2 = \kappa k_0^2 - (\kappa/\kappa_y)\gamma_n^2 \quad (16b)$$

and $p^2 = k_0^2 - \omega^2 - u_n^2$ for $y > h$, as in the case of $G_{x,z}$, while $\gamma_n^2 = u_n^2 + \omega^2$. Performing the required calculations to solve for the unknown coefficients $A_{1,2,3n}$ for Φ will result in the following expression which is analogous to (13) in [9]

$$\begin{aligned} H_n(\omega) = & (k_0^2/\gamma_n^2) \cdot (\rho_n \cdot \sin (pc) \\ & \cdot \sin (l_1 y)/\epsilon_0(p \cdot \sin (l_1 h) \cdot \cos (pc) + l_1 \\ & \cdot \cos (l_1 h) \cdot \sin (pc))) \\ & + (l_2 p/\gamma_n^2) \cdot (\rho_n \cdot \sin (pc) \\ & \cdot \sin (l_2 y)/\epsilon_0(p \kappa \cdot \sin (pc) \cdot \cos (l_2 h) + l_2 \\ & \cdot \cos (pc) \cdot \sin (l_2 h))). \end{aligned} \quad (17)$$

Performing the required contour integration to calculate the inverse Fourier Transform for Φ involving the expression $\int_{-\infty}^{\infty} H_n(\omega) e^{j\omega(z-z')} d\omega$, and noting that $dl_1/d\omega = -\omega/l_1$ while $dl_2/d\omega = -(\kappa/\kappa_y)\omega/l_2$ allows for the appropriate Green's function for the potential to be expressed as

$$\begin{aligned} G(x, h, z; x', h, z') = & (1/\epsilon_0 a) \sum_{n=1}^{\infty} \sum_{m=0}^{\infty} \cos (u_n x') \cdot \cos (u_n x') \\ & \cdot \{k_0^2 \cdot F(m) \cdot \exp [-\gamma_{nm}|z-z'|] / \\ & ((k_0^2 - p_m^2) \cdot \gamma_{nm}) \\ & - FB(m) \cdot \exp [-\bar{\gamma}_{nm}|z-z'|] / \\ & ((k_0^2 - \bar{p}_m^2) \cdot \bar{\gamma}_{nm})\} \end{aligned} \quad (18a)$$

where

$$\begin{aligned} F(m) = & l_m^2 \cdot p_m \cdot \sin^2 (l_m h) \cdot \sin^2 (p_m c) / (l_m^2 \cdot p_m \\ & \cdot (h \cdot \sin^2 (p_m c) + c \cdot \sin^2 (l_m h)) \\ & - (\kappa - 1) \cdot k_0^2 \cdot \sin^2 (l_m h) \cdot \sin (p_m c) \\ & \cdot \cos (p_m c)). \end{aligned} \quad (18b)$$

$$\begin{aligned} FB(m) = & \bar{l}_m^2 \cdot \bar{p}_m^2 \cdot \sin (\bar{l}_m h) \cdot \sin (\bar{p}_m c) / \{\bar{l}_m^2 \cdot c \\ & + \kappa_a \cdot \kappa \cdot \bar{p}_m^2 \cdot h) \cdot \sin (\bar{p}_m c) \cdot \sin (\bar{l}_m h) \\ & - \bar{p}_m \cdot \bar{l}_m \cdot (\kappa \cdot c + \kappa_a \cdot h) \cdot \cos (\bar{p}_m c) \\ & \cdot \cos (\bar{l}_m h) - \kappa \cdot \bar{l}_m \cdot \sin (\bar{p}_m c) \cdot \cos (\bar{l}_m h) \\ & - \kappa_a \cdot \bar{p}_m \cdot \sin (\bar{l}_m c) \cdot \cos (\bar{p}_m h)\}, \end{aligned} \quad (18c)$$

where $\kappa_a = \kappa_y/\kappa$. The $\gamma_{nm} = (u_n^2 + l_m^2 - \kappa k_0^2)^{1/2}$ and $\bar{\gamma}_{nm} = (u_n^2 + \kappa_a \cdot \bar{l}_m^2 - \kappa_y k_0^2)^{1/2}$ are the evanescent waveguide propagation constants, while the l_m , p_m , \bar{l}_m , and \bar{p}_m are the LSE and LSM eigenvalues, respectively, of the cut-off

waveguide. These eigenvalues are related by the expressions

$$l_m^2 - p_m^2 = (\kappa - 1)^2 \quad \text{for the LSE eigenvalues.} \quad (19a)$$

$$\kappa_a \cdot \bar{l}_m^2 - \bar{p}_m^2 = (\kappa_y - 1)^2 \quad \text{for the LSM eigenvalues.} \quad (19b)$$

Note that when $\kappa_y = \kappa$, the above expressions become the same as for the isotropic case. Notice that the effect of the anisotropy is to change the LSM eigenvalues compared to those obtained for the isotropic case.

The final expressions for the remaining Green's functions for a dielectric loaded waveguide of infinite extent now become

$$\begin{aligned} G_{x,z}(x, h, z; x', h, z') = & (1/a) \sum_{n=1}^{\infty} \sum_{m=0}^{\infty} \varphi_n(x, x') \cdot \exp [-\gamma_{nm}|z-z'|] \\ & \cdot F(m)/\gamma_{nm}, \end{aligned} \quad (20)$$

where $F(m)$ is defined in (18b), $\varphi_n(x, x')$ is defined in (12), and $G(x, h, z; x', h, z')$ is defined in (18).

With the Green's functions so obtained, the components of the electric field can be obtained from the potentials given in (6) and (7), as

$$E_x = -j\omega A_x - \partial\Phi/\partial x, \quad E_y = -j\omega A_y - \partial\Phi/\partial y$$

and

$$E_z = -j\omega A_z - \partial\Phi/\partial z \quad (21)$$

where it is required that for this geometry E_x and E_z vanish on the microstrip. The fields thus obtained are expressed in terms of the LSE and LSM (with respect to y) modes of the dielectric loaded waveguide. The anisotropic effect appears only in the LSM mode terms, which are present in A_y and Φ . The LSE waveguide modes are unchanged from those obtained for the isotropic case.

A complete set of dominant mode sources on the microstrip are represented: the longitudinal and transverse currents, as well as the charge on the microstrip line, with appropriate edge conditions built in. Over the useful operating range of most microstrip discontinuities, the amplitude of the transverse current, J_x , is very small relative to that of J_z and ρ , since the discontinuity is charge dominated under such circumstances. The effect of J_x becomes more pronounced for wide strips ($w/h \geq 5$) as the frequency is increased. Therefore, for a wide range of practical open end discontinuities, a valid approximation is to take $J_x = 0$, so therefore, $A_x = 0$. As a result, only the boundary condition $E_z = 0$ needs to be satisfied for this problem.

A line terminated at $z = 0$, forming an open end, would create reflected dominant mode sources on the line, along with perturbed sources localized near the discontinuity. The total source distribution on an open end discontinuity

may be written as,

$$J_z(x', h, z') = J_{0z}(x')(e^{-j\beta z'} - \text{Re}^{+j\beta z'}) + J_{1z}(x', z') \quad (22)$$

$$\rho(x', h, z') = \rho(x')(e^{-j\beta z'} + \text{Re}^{+j\beta z'}) + \rho(x', z'), \quad (23)$$

for $z' \leq 0$, where R is an unknown reflection coefficient, and J_{1z} and ρ_1 represent the perturbed source amplitudes near the open end.

An excellent representation for the x dependence of the sources on the microstrip line can be given in terms of weighted Chebychev polynomials, $T_{2i}(x/w)$. $(1 - (x/w))^{-1/2}$ where w is the microstrip width. Using the change of variable $x = w \sin \Theta$, the sources may be expressed as

$$J_z(\Theta') = \sum_{i=0}^{\text{IMAX}} l_i \cos(2i\Theta') / \cos \Theta' \quad (24a)$$

$$\rho(\Theta') = \sum_{i=0}^{\text{IMAX}} Q_i \cos(2i\Theta') / \cos \Theta' \quad (24b)$$

$$J_{1z}(\Theta', z') = j \sum_{i=0}^{\text{IMAX}} \sum_{k=0}^{\text{KMAX}} k_i \cos(2i\Theta') T_k(z') / \cos \Theta' \quad (24c)$$

$$\rho_1(\Theta', z') = \sum_{i=0}^{\text{IMAX}} \sum_{k=0}^{\text{KMAX}} D_{ki} \cos(2i\Theta') P_k(z') / \cos \Theta' \quad (24d)$$

where l_i and Q_i are the yet to be determined dominant mode current and charge amplitudes for an infinite line, and C_{ki} and D_{ki} are the unknown perturbed amplitudes. The Chebychev polynomials are used to express the source dependence in x for both dominant and perturbed sources, while triangle and pulse functions, $T_k(z')$ and $P_k(z')$, respectively, are used to represent the perturbed sources in z . When there is no transverse current ($J_x = 0$) on the microstrip line, the unknown charge amplitudes D_{ki} may be expressed directly in terms of the current amplitudes C_{ki} by the continuity equation, thus reducing the number of unknown by a factor of two. A modified perturbation technique, based on the technique developed in [9] is used to determine the l_i , Q_i and β for the infinitely long microstrip line.

Equations (22) and (23) may be written as

$$J_z(x', h, z') = j(1 + R) J_{0z}(x')(B_{in} \cos(\beta z') - \sin(\beta z')) + J_{1z}(x', z') \quad (25)$$

$$\rho(x', h, z') = (1 + R)\rho_0(x')(B_{in} \sin(\beta z') + \cos(\beta z')) + \rho_1(x', z') \quad (26)$$

where $jB_{in} = (1 - R)/(1 + R)$ is the normalized input susceptance for the open end. Since the perturbed amplitudes J_{1z} and ρ_1 given in (24c) and (24d) are still arbitrary,

they may be defined so as to have the $(1 + R)$ term appear as a scale factor multiplying them as well. Since this makes the $(1 + R)$ term common to all source terms, it may be normalized to 1.0 with no loss of generality. For an open end, the potentials now become,

$$A_z = \mu_0 \int_{-w}^w \left\{ \int_{-\infty}^{\infty} j J_{0z}(x') (B_{in} \cos(\beta z') - \sin(\beta z')) G_z dz' + \int_{-\infty}^0 J_{1z}(x', z') G_z dz' \right\} dx' - \int_0^{\infty} j J_{0z}(x') (B_{in} \cos(\beta z') - \sin(\beta z')) G_z dz' \quad (27)$$

$$\Phi = \epsilon_0 \int_{-w}^w \left\{ \int_{-\infty}^{\infty} \rho_0(x') (B_{in} \sin(\beta z') + \cos(\beta z')) G dz' + \int_{-\infty}^0 \rho_1(x', z') G dz' \right. \\ \left. - \int_0^{\infty} \rho_0(x') (B_{in} \sin(\beta z') + \cos(\beta z')) G dz' \right\} dx'. \quad (28)$$

Substituting (27) and (28) into (21) gives the electric field in terms of the sources on the open end microstrip line. When the requirement that $E_z = 0$ on the microstrip is enforced, the terms corresponding to the dominant mode on the infinite line already satisfy the boundary condition on the strip, so they drop out. The sources existing for $z' > 0$ may be considered "source reversed" terms which produce an impressed field in the region $z \leq 0$, but localized near the discontinuity. Because they have known amplitudes, these dominant mode sources make up a known forcing function. The electric field produced by the perturbed sources J_{1z} and ρ_1 , must cancel the tangential component of the applied field for $z \leq 0$. The method of moments is then used to reduce the resulting integral equation to a matrix equation which can be solved for the unknown input admittance B_{in} , as well as for J_{1z} and ρ_1 . Only one matrix inversion is required to find B_{in} .

Unweighted Chebychev polynomials are used to test the resulting equations along x rather than the weighted polynomials, so as not to overemphasize the contribution to the field from the sources at the edge of the microstrip. Testing along z was performed using pulse functions. The resulting integrals can all be evaluated in closed form, so no numerical integration is required. Most of the double sums have terms involving exponential decay, so they converge rapidly. Only those terms which arise when the source and field points coincide have no exponential decay. Those terms, however, can all be summed over one of the indices (the m index), resulting in expressions involving only a single sum over n . These single sums can be further manipulated so that their dominant portions are summed into closed form, leaving only a correlation term to be calculated [9], [11]. In this fashion, slowly con-

verging series that might have required the evaluation of 90 000 or more terms ($n = m \approx 300$) to obtain a converged solution can be accurately evaluated with 25 to 30 terms instead.

RESULTS

Near the open end, the expansion pulses along z' used to represent the perturbation in the sources should have a narrow pulse width, since the dependence of the sources in this region will vary as $|z'|^{-1/2}$, while wider pulse widths should be used farther away from the open end. This need for expansion pulses of significantly different width can be accomplished by means of pulse compression, which is shown in Fig. 2 for triangle functions, where properly weighted unit pulses are combined to create wider pulses along with suitable transition pulses. The primary advantage of this approach is that this summation can be performed on the appropriate rows and columns of the coefficient matrix, so that the expansion and testing pulses used in evaluating the appropriate integrals can all be of equal ("unit") width. In this way, no special attention needs to be paid to the evaluation of the integrals involved in expansion and testing along the line. This results in a substantial computational savings in filling the coefficient array.

In generating these results, three modes ($IMAX = 2$ in (28)) each are used to expand the dominant and perturbed sources in x . With this representation, the amplitude of the $i = 2$ mode is usually $< 1\%$ of the $i = 0$ mode, with each succeeding mode smaller in amplitude by a factor of 10 than its preceding one. Consequently, any further increase in the number of modes beyond three provides no significant effect on the solution. For the z dependence, 27 unit pulses are associated with the $i = 0$ mode, which are compressed to 12 pulses. The $i = 1$ and 2 modes in x each have five expansion pulses in z associated with them. Due to the small number of pulses involved in the $i = 1$ and 2 modes, no pulse compression is used with them. On the open end, the total current in the z direction must be zero at $z = 0$. To accomplish this, the perturbed currents must cancel the dominant mode current, resulting in the relationship $I_i B_{in} + C_{1i} = 0$, or $C_{1i} = -B_{in} I_i$, where the C_{1i} are the unknown current amplitudes at the open end and the I_i are the known dominant mode amplitudes. This relationship reduces the number of unknowns used for this particular formulation to 19 source amplitudes along with B_{in} for a total of 20 unknowns, resulting in a 20 by 20 coefficient array. The number of expansion modes in x and/or z may be increased by simply changing the appropriate summation indices. In this way, the accuracy of the source representation may be increased to any required or desired level.

The unit pulse width, Δ (where $\Delta = 2 \cdot d$ in Fig. 2), of the expansion functions was chosen to be 0.32 mm at $f = 2.0$ GHz (or $\Delta \approx 0.0053\lambda_g$ for sapphire). This pulse width guaranteed a converged value for B_{in} [8] for all of the examples presented. To verify the accuracy of the the-

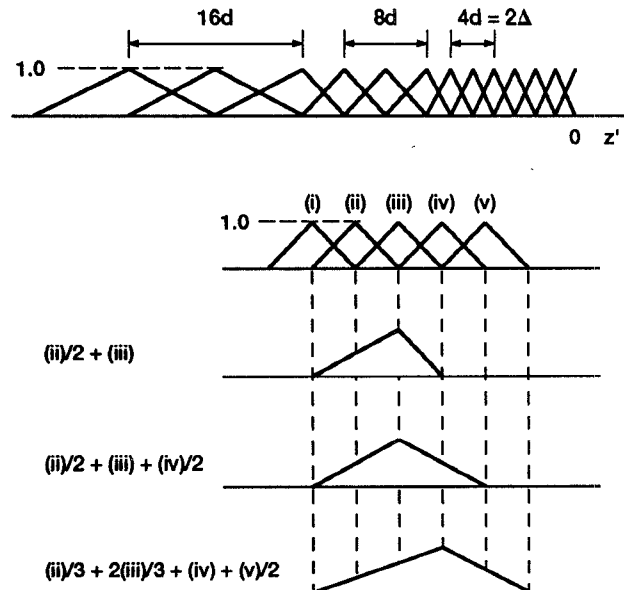


Fig. 2. Pulse compression along the microstrip line. For clarity, only the triangle pulses are shown.

ory, as well as the resulting program, the program was checked for the isotropic dielectric case, and was able to duplicate data obtained in [2] and [8]. A further check was to examine the dominant mode source amplitudes for an infinite line using this technique with those determined from a computer program developed on the basis of [9]. The sidewall spacing was kept the same as in [9] while the placement of the top cover was varied from $10 \cdot h$ to $12 \cdot h$, thus simulating an open structure. Using these dimensions for the waveguide, there was practically no difference observed in the resulting dominant mode amplitudes for an infinite line enclosed with sidewalls but no top cover. Since placement of the top cover at a height of $10 \cdot h$ above the substrate was found to be suitable, this value was used throughout.

Table I shows the results obtained using this technique for several different anisotropic substrates as a function of microstrip linewidth. The open circuit capacitance, C_{oc} is found using $C_{oc} = B_{in}/\omega Z_0$, where the characteristic impedance Z_0 is obtained from [9], for an infinite microstrip line with sidewalls but no top cover. Calculations of Z_0 performed for a microstrip line on an air dielectric ($\epsilon_1 = 1.0$) with and without a top cover gave values of Z_0 that differed by less than 2% for strip widths ranging from $w/h = 0.25$ to 6.0 and frequencies up to 10 GHz, so the use of Z_0 values obtained from [9] is justified.

Table II shows the variation of C_{oc} as a function of line width for sapphire, and compares the results obtained for a substrate with an isotropic dielectric constant of 9.4, as well as for an isotropic dielectric constant of 11.6. Table III shows the effects of fixed waveguide dimensions on B_{in} and C_{oc} as a function of frequency of the propagating microstrip mode. For low frequencies, B_{in} varies linearly with frequency, starting to deviate as the frequency increases. This effect becomes more pronounced until the cut off frequency of the E_{11} waveguide mode is reached.

TABLE I

OPEN CIRCUIT CAPACITANCE, C_{oc} , FOR SEVERAL ANISOTROPIC DIELECTRIC MATERIALS. FREQ. = 2.0 GHz, $h = 1.0$ mm, $b = 11$ mm, $2a = 20$ mm FOR $W/h < 4.0$, ELSE $2a = 10 (W/h)$. Z_0 VALUES OBTAINED FROM [8]. UNITS ARE pF/METER FOR C_{oc}

	$W/h =$	0.25	0.5	1.0	2.0	4.0	6.0
PTFE/Woven glass	κ_e	1.914	1.941	1.981	2.042	2.129	2.182
$\kappa = 2.84$	Z_0	150.5	119.9	90.02	62.46	39.82	29.50
$\kappa_y = 2.45$	C_{oc}/W	29.85	23.71	19.90	17.66	16.29	15.60
Boron Nitride	κ_e	2.676	2.699	2.738	2.808	2.922	2.999
$\kappa = 5.12$	Z_0	127.4	101.7	76.68	53.38	34.09	25.25
$\kappa_y = 3.4$	C_{oc}/W	43.04	33.95	28.27	24.84	22.72	21.66
Sapphire	κ_e	6.724	4.012	7.647	8.145	9.007	9.514
$\kappa = 9.4$	Z_0	80.90	63.65	46.94	31.82	19.80	14.52
$\kappa_y = 11.6$	C_{oc}/W	80.36	65.56	56.38	50.95	47.43	45.35
Epsilam 10	κ_e	6.885	7.047	7.306	7.721	8.308	8.679
$\kappa = 13$	Z_0	79.90	63.44	47.39	32.61	20.55	15.14
$\kappa_y = 10.3$	C_{oc}/W	95.28	76.26	64.44	57.35	52.93	50.49

TABLE II

VARIATION OF C_{oc} AS A FUNCTION OF LINE WIDTH FOR SAPPHIRE, $\kappa = 9.4$, $\kappa_y = 11.6$ COMPARED TO THAT OF AN ISOTROPIC DIELECTRIC. FREQ. = 2.0 GHz, $h = 1.0$ mm, $b = 11$ mm, $2a = 20$ mm FOR $W/h < 4.0$, ELSE $2a = 10 (W/h)$. UNITS ARE pF/METER FOR C_{oc}

	$W/h =$	0.25	0.5	1.0	2.0	4.0	6.0
Sapphire							
$\kappa = 9.4$	$C_{oc}/W =$	80.36	65.56	56.38	50.95	47.43	45.35
$\kappa_y = 11.6$							
$\kappa = 9.4$	$C_{oc}/W =$	75.56	61.06	52.10	46.80	43.42	41.52
$\kappa_y = 9.4$							
$\kappa = 11.6$	$C_{oc}/W =$	90.18	73.27	62.58	56.21	52.13	49.77
$\kappa_y = 11.6$							

TABLE III

VARIATION OF THE NORMALIZED INPUT SUSCEPTANCE, B_{in} , AND OPEN CIRCUIT CAPACITANCE, C_{oc} , WITH FREQUENCY. WAVEGUIDE DIMENSIONS ARE $2a = 20$ mm, $b = 11$ mm, $h = 1$ mm, $w = 1$ mm ($w/h = 1.0$)

Freq. (GHz)	B_{in}	C_{oc} (pF/m)
0.5	.008388	56.26
1.0	.016776	56.26
2.0	.033256	56.38
4.0	.068373	56.85
6.0	.167738	90.81

This effect may be overcome by either frequency scaling the input parameters or by adjusting the waveguide dimensions accordingly. Alternately, once C_{oc} is obtained at a low frequency, the corresponding value of B_{in} can be calculated at the desired frequency. The computer program developed to implement this technique was done in compiled BASIC, requires less than 640 K of RAM, and can run on a personal computer. When executed on an Epson Equity II operating at a clock rate of 7.16 MHz, the compiled code will compute B_{in} for an open end discontinuity in under three minutes per frequency point. This includes the time required to find the first 100 LSE and LSM eigenvalues for a dielectric loaded waveguide, the dominant mode propagation constant, β along with the dominant mode charge, and current amplitudes for an infinite microstrip line. Another factor that increased the execution time is that some variables had to be recalcula-

lated many times during a particular run, since extra array space that would be required for their storage could not be defined while remaining within the available block size. An in-line compiler could have significantly reduced the run time for the program but could not be used with this program since it generated a code that was substantially larger than the personal computer of this particular generation could handle. Clearly significant performance gains can be obtained simply by executing the program on a more powerful platform and using a more efficient language, other than BASIC.

Regardless of the platform used, further speed improvements are obtained when only the microstrip line-width is varied for a given substrate thickness and frequency. In this way, the program can be repeatedly executed to calculate B_{in} , with the advantage that many variables need not be recalculated each time; specifically, the LSE and LSM mode eigenvalues need to be calculated only once in this case.

This technique can be extended to rapidly and accurately characterize a number of other commonly used discontinuity structures, especially "coaxial" two port structures such as asymmetrical gaps and steps in width. To characterize a two port structure in terms of an equivalent "Tee" or "Pi" network, the Tangent Plane method [10] can be used to extract equivalent circuit parameter values based on three distinct B_{in} values obtained with a movable shorting plane located at a suitable distance from the junction in question. Dielectric loss could also be in-

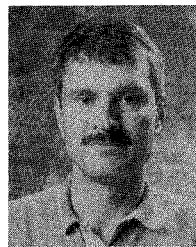
cluded in this technique, although the effect of dielectric loss is more significant when determining the propagation constant of a microstrip line than in determining the open circuit capacitance.

CONCLUSIONS

Microstrip open end discontinuities patterned on anisotropic dielectric substrates have been characterized in terms of their normalized input susceptance and open circuit capacitance using a dynamic source reversal technique based on potential theory. The technique allows for all of the sources on the discontinuity structure to be represented with proper edge conditions built in. The effects of an enclosure on the discontinuity can be simulated by a proper spacing of the sidewalls and top cover of the waveguide enclosure. The BASIC computer program developed to implement this technique can be executed on a personal computer with as little as 640 K of RAM. The technique is computationally efficient, there is no need for a source excitation, and the admittance can be solved for directly in the case of a one port network. All integrals involving the expansion and testing functions are performed analytically so no numerical integrations are necessary and the dominant portion of slowly converging series can be extracted and summed into closed form. The technique can be expanded to characterize other commonly used microstrip discontinuities.

REFERENCES

- [1] R. E. Collin and S. Toncich, "Potential Theory for Microstrip Discontinuities," presented at the *URSI Nat. Radio Sci. Meet.*, Boulder, CO, Jan. 1989.
- [2] P. Silvester and P. Benedek, "Equivalent Capacitance of Microstrip Open Circuits," *IEEE Trans. Microwave Theory Tech.*, vol. 20, pp. 511-516, Aug. 1972.
- [3] P. Silvester and P. Benedek, "Equivalent Capacitance of Microstrip Gaps and Steps," *IEEE Trans. Microwave Theory Tech.*, vol. 20, pp. 729-733, Nov. 1972.
- [4] P. Anders and F. Arndt, "Microstrip Discontinuity Capacitances and Inductances for Double Steps, Mitered Bends with Arbitrary Angle, and Asymmetric Right Angle Bends," *IEEE Trans. Microwave Theory Tech.*, vol. 28, pp. 1213-1217, Nov. 1980.
- [5] R. H. Jansen, "Hybrid Mode Analysis of End Effects of Planar Microwave and Millimeter Wave Transmission Lines," *Proc. Inst. Elec. Eng. Pt. H*, vol. 128, pp. 77-86, 1981.
- [6] J. C. Rautio and R. F. Harrington, "An Electromagnetic Time Harmonic Analysis of Shielded Microstrip Circuits," *IEEE Trans. Microwave Theory Tech.*, vol. 35, pp. 726-731, Aug. 1987.
- [7] R. W. Jackson, "Full Wave, Finite Element Analysis of Irregular Microstrip Discontinuities," *IEEE Trans. Microwave Theory Tech.*, vol. 37, pp. 81-89, Jan. 1989.
- [8] S. S. Toncich and R. E. Collin, "Characterization of Microstrip Discontinuities by a Dynamic Source Reversal Technique Using Potential Theory," *14th Triennial URSI Int. Symp. on Electromag. Theory*, pp. 520-523, Sydney, Australia, 1992.
- [9] B. E. Kretch and R. E. Collin, "Microstrip Dispersion Including Anisotropic Substrates," *IEEE Trans. on Microwave Theory Tech.*, vol. 35, pp. 710-718, Aug. 1987.
- [10] R. E. Collin, *Field Theory of Guided Waves*, 2nd Ed. New York: IEEE Press, Ch. 5, 1991.
- [11] —, Mathematical appendix.



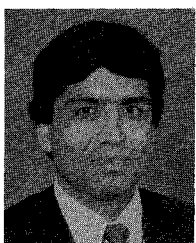
Stanley S. Toncich (M'88-SM'93) received the B.S., M.S., and Ph.D. degrees from Case Institute of Technology, Cleveland, OH, in 1977, 1981, and 1991, respectively.

From 1979 to 1981, he was an Engineer in the Receiver Engineering Department at Magnavox, Torrance, CA. From 1981 to 1982 he was in the Radar Systems Department at Martin Marietta Aerospace. From 1982 to 1984, he was a Senior Engineer at Lockheed Electronics, Orlando, FL. After receiving his Ph.D. he was National Research Council Fellow in the Space Electronics Division at the NASA Lewis Research Center in Cleveland, OH. From 1991 to 1993, he did research in the application of high temperature superconductivity to microwave communication system components. He is currently a Senior R&D Engineer at the Bird Electronic Corporation, Solon, OH, where his interests include passive microwave devices, directional couplers and rf/microwave power measurement techniques.

Robert E. Collin (M'54-SM'60-F'72) was born in Alberta, Canada, in 1928. He received the B.Sc. degree in engineering physics from the University of Saskatchewan in 1951, attended Imperial College in England for graduate work, and received the Ph.D. degree in electrical engineering from the University of London in 1954.

From 1954 to 1958 he was a Scientific Officer at the Canadian Armament Research and Development Establishment. He was also an Adjunct Professor at Laval University during this time. He immigrated to the United States in 1958 and became a citizen in 1964. He joined the Department of Electrical Engineering at Case Institute of Technology (now Case Western Reserve University), Cleveland, OH, in 1958. During his tenure there, he has served as Chairman of the Department of Electrical Engineering and Applied Physics for five years, and also as Interim Dean of Engineering for two years. He has been an Invited Professor at the Catholic University in Rio de Janeiro, Brazil; at Telebras Research Center, Campinas, Brazil; and the University of Beijing, People's Republic of China. He was also a Distinguished Visiting Professor at the Graduate School, Ohio State University, Columbus, during the 1982-1983 academic year. He is the author/coauthor of more than 100 technical papers. He is also the author of *Field Theory of Guided Waves, Foundations for Microwave Engineering, Antennas and Radiowave Propagation*, a coauthor with R. Plonsey of *Principles and Applications of Electromagnetic Fields*, and coeditor with F. Zucker and contributing author of *Antenna Theory, Parts I and II*.

Dr. Collin is a member of the National Academy of Engineering, the IEEE Antennas and Propagation Society, the IEEE Microwave Theory and Techniques Society, and the USA Commission B of URSI. He has served on a variety of IEEE Committees for Awards, Publications, Technical Programs, and Standards.



Kul B. Bhasin (SM'89) received the M.S. degree from Purdue University, West Lafayette, IN, and the Ph.D. degree from the University of Missouri-Rolla.

From 1977 to 1983, he was a Senior Scientist and Manager of Technology with Gould, Inc. Since 1983 he has been a Senior Research Scientist in the Solid State Technology Branch of the Space Electronics Division of the NASA Lewis Research Center, Cleveland, OH. He is currently engaged in development of GaAs microwave devices and circuits, microwave photonics, and superconducting electronics for space applications.

Dr. Bhasin is a member of APS, Sigma Xi, and a Fellow International Society for Optical Engineers. He is the recipient of the IR-100 Award, the NASA Group Achievement Awards, and the Gould Scientific Achievement Award. He is on the editorial board of *Microwave and Optical Technology Letters*.